ChemComm

COMMUNICATION

View Article Online
View Journal | View Issue

A photothermal cell viability-reporting theranostic nanoprobe for intraoperative optical ablation and tracking of tumors†

Cite this: *Chem. Commun.*, 2014, **50**, 8014

Received 11th March 2014,
Accepted 1st May 2014

DOI: 10.1039/c4cc01823k

www.rsc.org/chemcomm

Shuqi Wu,[a] Shoufa Han,*[a] Jiahuai Han[b] and Xinhui Su*[c]

A photothermal pH-reporting nanoprobe was developed for intraoperative tumor detection by "turn-on" fluorescence of the probe inside viable tumor cells, photothermal tumor therapy, and *in situ* monitoring of tumor killing by non-fluorescence of the probe in damaged cells.

Surgical resection is widely used in the treatment of solid tumors. Incomplete removal of tumor foci, due to limited visibility of disseminated or tiny tumor foci under visual inspection, results in tumor relapse. As such, optical probes that could guide surgeons to evasive tumor foci have been actively explored.[1] Optical systems that could be activated to fluorescence-on states inside tumors while being non-fluorescent in off-target settings are advantageous to achieve high tumor-to-background signal contrast.[2] Probes that can convert light energy into cytotoxic heat are promising tools for photothermal cancer therapy, which is non-invasive and could be administered in a controlled manner with the use of exogenous light.[3] In this context, near-infrared light (NIR)-absorbing polypyrrole (PPy), displaying a number of favorable characteristics, has been increasingly explored for photothermal therapy.[4] Despite the advances in fluorescence guided staging of evasive tumors, complete surgical removal of small-sized or disseminated tumors remains challenging. As such, alternative modalities that could be use to identify and kill tumors intraoperatively are of clinical significance.

We previously reported the use of acid activated rhodamine derivatives with intramolecular spiro-rings for fluorescence guided intraoperative detection of tumors in mice by proton triggered turn-on fluorescence within tumors.[5] Herein we report the use of a multifunctional nanoprobe, PPy@SiO_2@dRB, integrating photothermal PPy with acid-responsive *N*-(rhodamine B)-deoxylactam (dRB) for fluorescence guided tumor detection and photothermal killing of tumors (Fig. 1). PPy@SiO_2@dRB features a hydrophilic corona of polyethylene glycol, a silica shell decorated with dRB and an inner core of PPy. Acidic lysosomal pH is maintained in viable cells by V-ATPase mediated proton pumping, and is dissipated upon cell death. The fluorescence-off of PPy@SiO_2@dRB within damaged cells due to the disruption of lysosomal pH homeostasis was employed for *in situ* monitoring of photothermal effects on targeted tumors.

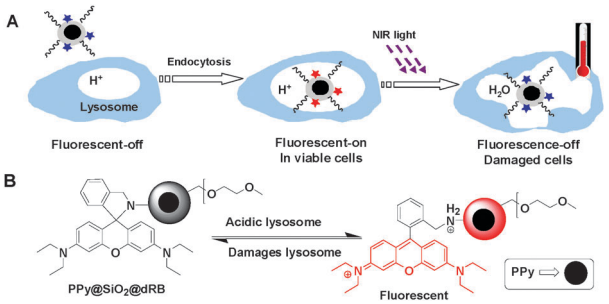

Fig. 1 (A) Illustration of fluorescence guided tumor detection, photothermal destruction and tracking of responses of tumors with PPy@SiO_2@dRB. (B) Surface-anchored dRB isomerizes into fluorescent species within acidic lysosomes and reverts to the non-fluorescent state upon loss of lysosomal acidity at cell death.

Light is non-invasive and can be manipulated for biomedical applications in a spatio-temporally controlled manner. Given the limited tissue penetration of external light, we envision that the combination of phototherapy with tumor surgery would be of practical utility owing to exposure of tumor-bearing tissues that are otherwise inaccessible to light. As biological tissues are have the least absorption in the NIR region, NIR-absorbing PPy was used as the photothermal agent to conjugate with pH-responsive dRB for fluorescence guided tumor detection. As PPy is a fluorescence quencher,

[a] *Department of Chemical Biology, College of Chemistry and Chemical Engineering, Key Laboratory for Chemical Biology of Fujian Province, MOE Key Laboratory of Spectrochemical Analysis & Instrumentation, Innovation Center for Cell Biology, Xiamen University, Xiamen 361005, China. E-mail: shoufa@xmu.edu.cn*
[b] *State Key Laboratory of Cellular Stress Biology, Innovation Center for Cell Biology, School of Life Sciences, Xiamen University, Xiamen 361005, China*
[c] *Department of Nuclear Medicine, Zhongshan Hospital, Xiamen University, Xiamen 361004, China. E-mail: suxinhuii@163.com; Tel: +86-0592-2181728*

† Electronic supplementary information (ESI) available: Experimental procedures; synthesis and characterization of PPy@SiO_2@dRB and SiO_2@dRB; effects of NIR irradiation on the fluorescence of SiO_2@dRB within cells; cytotoxicity of PPy@SiO_2@dRB. See DOI: 10.1039/c4cc01823k

it is critical that the conjugated dRB remains emissive within cells. To physically separate PPy and dRB, nanoscale PPy prepared by ferric chloride mediated polymerization[6] was first coated with a silica shell *via* condensation with tetraethoxysilane to give PPy@SiO_2, which was further functionalized with dRB conjugated triethoxysilane (dRB-PTS) and 3-aminopropyltriethoxysilane (APTS) to introduce the dRB profluorophore and amino moieties onto the surface (Scheme S1, ESI†). To increase the colloidal stability and decrease *in vivo* recognition by the reticuloendothelial systems, the as-prepared particles were modified with polyethylene glycol to afford PPy@SiO_2@dRB which was used for *in vitro* cell studies and *in vivo* tumor targeting.

Scanning electron microscopy (SEM) images show that PPy@SiO_2@dRB has a uniform diameter of 100 nm, whereas that of PPy is 50 nm (Fig. 2A), which is consistent with dynamic light scattering analysis (Fig. S1, ESI†). Zeta potential analysis showed that the surface potentials decreased from 6.9 mV to −3.8 mV after PEGylation of PPy@SiO_2@dRB (ESI,† Fig. S2). These results confirm the formation of silica shells around PPy. To probe its pH responsiveness, PPy@SiO_2@dRB was spiked into buffers of various pH values, and the fluorescence emission was recorded over buffer pH. As shown in Fig. 2B, PPy@SiO_2@dRB, which is weakly fluorescent in neutral or alkaline conditions, exhibits a strong emission centered at 590 nm which intensifies as the buffer pH decreases. The pK_a of the dRB entity was estimated to be 6.5. Analysis of the solutions by UV-vis-NIR spectroscopy showed that PPy@SiO_2@dRB displays characteristic absorbance of rhodamine B under acidic pH (Fig. 2C), further proving the presence of dRB on the silica shells. Compared with SiO_2@dRB without PPy, PPy@SiO_2@dRB displays significant absorbance at 650–900 nm (Fig. 2D), suggesting its capability to absorb NIR light. Aqueous solutions spiked with various amounts of PPy@SiO_2@dRB were exposed to 808 nm laser illumination at a power density of 2 W cm^{-2}. The solutions displayed dose- and irradiation time-dependent temperature elevation (Fig. 2E), showing that PPy@SiO_2@dRB could effectively convert NIR light into heat.

Lysosomes are acidic subcellular vesicles where the acidity is maintained in viable cells by V-ATPase mediated pumping of proton into lysosomes driven by ATP hydrolysis. To probe lysosomal pH mediated fluorescence, HeLa, HepG2 and 4T1 cells were respectively cultured with PPy@SiO_2@dRB in medium spiked with LysoTracker Green DND-26 (referenced to as Lysotracker green). No obvious fluorescence was identified in the cells or culture medium immediately after the addition of PPy@SiO_2@dRB. Upon incubation, confocal microscopic images show that rhodamine fluorescence can be clearly identified within all the cell lines tested, and colocalizes with Lysotracker green which is a lysosome specific dye (Fig. 3), showing that the probe becomes fluorescent upon internalization into lysosomes. To assess the effects of lysosomal acidity on dRB fluorescence, we measured signals of PPy@SiO_2@dRB in cells treated with Bafilomycin A1 (BFA), which inhibits the activity of V-ATPase and alkalinizes lysosomal pH.[7] The intracellular fluorescence largely

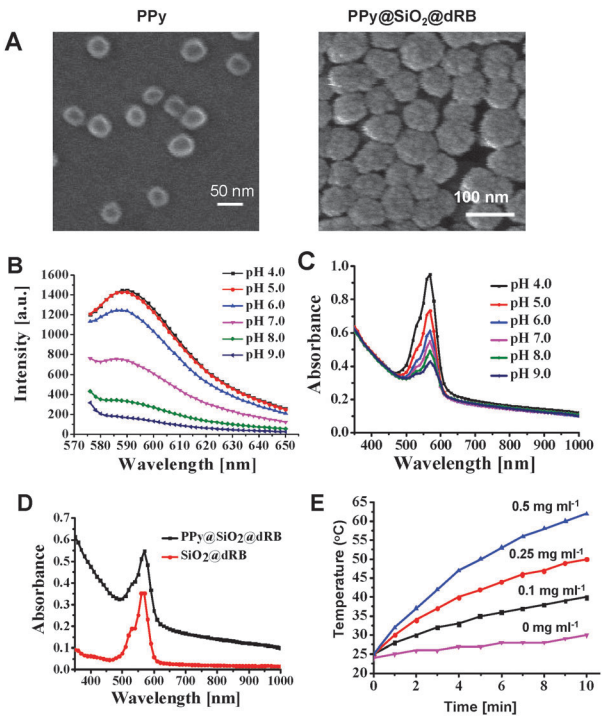

Fig. 2 Characterization of PPy@SiO_2@dRB. (A) SEM images of PPy and PPy@SiO_2@dRB; (B) fluorescence emission of PPy@SiO_2@dRB (50 μg ml^{-1}) in sodium phosphate buffer solutions (pH 4.0–9.0, λ_{ex} = 560 nm); (C) UV-vis-NIR absorption spectra of PPy@SiO_2@dRB (50 μg ml^{-1}) in sodium phosphate buffer solutions (pH 4.0–9.0); (D) UV-vis-NIR absorption of PPy@SiO_2@dRB (50 μg ml^{-1}) and SiO_2@dRB (50 μg ml^{-1}) in sodium phosphate buffer solution (pH 7.0); (E) the temperature of water containing PPy@SiO_2@dRB (0–0.5 mg ml^{-1}) upon irradiation with a NIR laser (808 nm, 2 W).

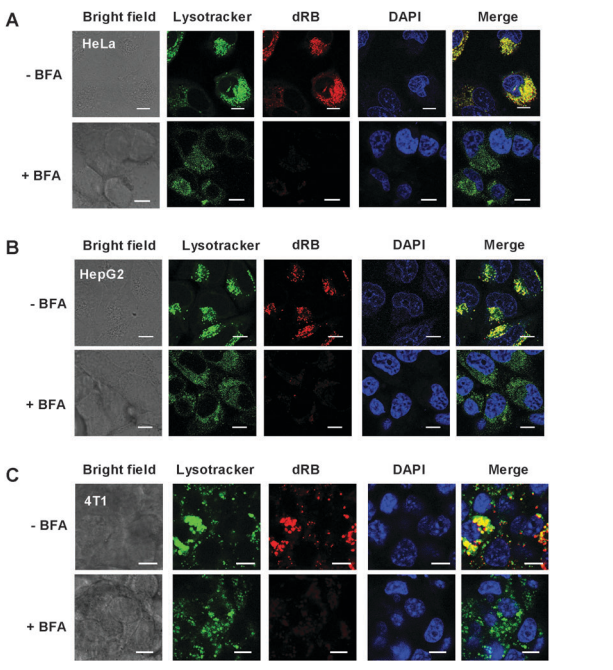

Fig. 3 Lysosomal pH dependent fluorescence of PPy@SiO_2@dRB. HeLa (A), HepG2 (B) and 4T1 cells (C) treated with or without BFA (50 nM) were respectively cultured in Dulbecco's modified Eagle's medium (DMEM) supplemented with PPy@SiO_2@dRB (50 μg ml^{-1}) and 4′,6-diamidino-2-phenylindole (DAPI) (1 μM) for 2 h, and then stained with Lysotracker green (1 μM) for 30 min. The cells were visualized by confocal fluorescence microscopy. Colocalization revealed by overlay of the dRB signals (shown in red) with the Lysotracker green signals (shown in green) is indicated by the yellow areas. Scale bars: 5 μm.

vanished in BFA-treated cells (Fig. 3), confirming the lysosomal acidity dependent "turn-on" signal of PPy@SiO_2@dRB within cells.

Having been demonstrated to be luminescent within acidic lysosomes, PPy@SiO_2@dRB was evaluated for its feasibility to report cell death. HeLa, 4T1 and HepG2 cells were respectively cultured with PPy@SiO_2@dRB or SiO_2@dRB and then either irradiated with a NIR laser or not irradiated. No obvious fluorescence changes were observed in control cells treated with NIR light and SiO_2@dRB (Fig. S3, ESI†). In contrast, the intracellular fluorescence largely disappeared in all the cell lines treated with PPy@SiO_2@dRB and NIR illumination (Fig. 4), demonstrating the PPy dependent fluorescence-off upon NIR irradiation. As dRB fluorescence is dependent on lysosomal acidity (Fig. 3), these results suggest disruption of lysosomal pH by heat generated from the NIR laser with the aid of PPy@SiO_2@dRB. A cell viability assay using 3-(4,5-dimethylthiazol-2-yl)-2,5-diphenyltetrazolium (MTT) reveals significant cell death in the three cell lines treated with NIR light and PPy@SiO_2@dRB, whereas the viability of cells treated with the NIR laser (808 nm, 2 W) or PPy@SiO_2@dRB alone was largely unaffected (Fig. 4E). In control experiments, no detrimental effects were observed on the viability of HeLa, 4T1 and HepG2 cells treated with SiO_2@dRB and NIR irradiation (ESI,† Fig. S3). These results establish the synergistic effects of PPy@SiO_2@dRB and NIR irradiation for effective photothermal killing of targeted cells. Collectively, the NIR irradiation-triggered decrease of intracellular fluorescence validates the use of PPy@SiO_2@dRB for reporting of cell death.

With the cell death correlated signal-off of PPy@SiO_2@dRB (Fig. 4), we explored its potential for intraoperative photothermal tumor therapy in mice models. 4T1 mouse breast carcinoma cells were subcutaneously injected into the flank of female Balb/c mice.

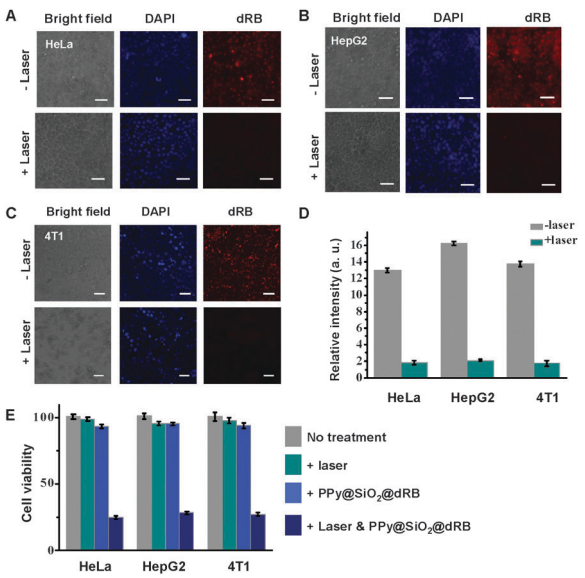

Fig. 4 NIR irradiation-mediated signal-off of PPy@SiO_2@dRB within cells. HeLa (A), HepG2 (B) and 4T1 cells (C) were respectively cultured for 6 h in DMEM spiked with or without PPy@SiO_2@dRB (50 μg ml^{-1}), and then either irradiated with a NIR laser or not irradiated in fresh DMEM for 10 min. The cells were analyzed by fluorescence microscopy and MTT assay; (D) intracellular fluorescence emission of dRB at 575–590 nm was collected using λ_{ex} = 510–560 nm; (E) cell viability was determined by MTT assay. Scale bars: 50 μm.

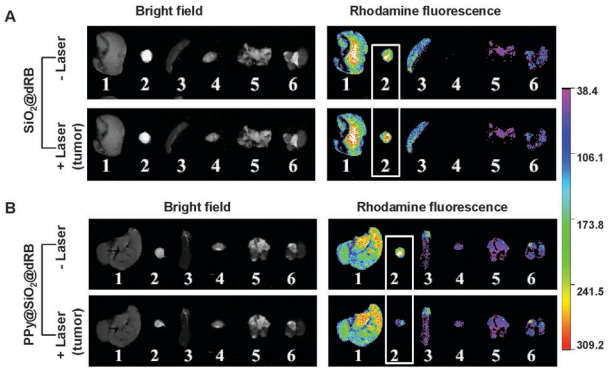

Fig. 5 NIR irradiation mediated fluorescence attenuation of PPy@SiO_2@dRB in subcutaneous tumors. Balb/c mice with subcutaneous tumors were intravenously injected with SiO_2@dRB (30 mg kg^{-1}) (A) or PPy@SiO_2@dRB (30 mg kg^{-1}) (B) *via* the tail vein and then sacrificed 12 h postinjection. The representative organs and tumors were dissected and imaged by *ex vivo* fluorescence analysis. The tumors were either irradiated with a NIR laser for 5 min or not irradiated and then imaged for tumor-associated fluorescence in parallel with the organs without NIR irradiation. The organs are arranged in the following sequence: liver (1), tumor (2), spleen (3), heart (4), lung (5), and kidney (6).

5–10 days after the xenograft, PPy@SiO_2@dRB and SiO_2@dRB were respectively injected *via* the tail vein into the bloodstreams of the tumor-bearing mice. The mice were sacrificed 12 h postinjection, and the subcutaneous tumors were dissected and irradiated with a NIR laser for 5 min. *Ex vivo* fluorescence images revealed strong rhodamine fluorescence in the subcutaneous tumors from both the mice treated with PPy@SiO_2@dRB and those treated with SiO_2@dRB (Fig. 5), showing that these probes could effectively accumulate and become luminescent in tumors, thus proving their utility for fluorescence-guided intraoperative tumor detection. To our delight, the tumors from the mice treated with PPy@SiO_2@dRB displayed marked fluorescence attenuation upon *ex vivo* NIR irradiation, whereas no obvious signal changes were observed in the tumors from mice injected with SiO_2@dRB under identical treatment (Fig. 5). The difference clearly validates the feasibility of tracking photothermal effects on tumors with PPy@SiO_2@dRB during surgery.

In summary, photothermal and acid activated PPy@SiO_2@dRB was prepared and was shown to become fluorescent within acidic lysosomes upon cellular internalization. Efficient cell death was induced by NIR irradiation and the endocytosed PPy@SiO_2@dRB, leading to fluorescence-off of the probe in cells and subcutaneous tumors owing to the heat-triggered loss of functional lysosomal pH in damaged cells. Photothermal PPy@SiO_2@dRB, with cell viability-reporting optical read-out, would be of potential use for fluorescence-guided intraoperative tumor detection, photothermal killing of surgically exposed tumors, and *in situ* tracking of the effects of photothermal therapy during surgical tumor treatment.

Dr S. Han was supported by grants from the 973 program (2013CB93390), NSFC (21272196), the Fundamental Research Funds for the Central Universities (2012121018), NSF of Fujian Province (2011J06004), and PCSIR; Dr X. Su was supported by grants from NSFC (81071182) and the Medical Innovation Foundation of Fujian (2009-CXB-46).

Notes and references

1 (*a*) Y. Urano, D. Asanuma, Y. Hama, Y. Koyama, T. Barrett, M. Kamiya, T. Nagano, T. Watanabe, A. Hasegawa, P. L. Choyke and H. Kobayashi, *Nat. Med.*, 2009, **15**, 104; (*b*) G. M. van Dam, G. Themelis, L. M. Crane, N. J. Harlaar, R. G. Pleijhuis, W. Kelder, A. Sarantopoulos, J. S. de Jong, H. J. Arts, A. G. van der Zee, J. Bart, P. S. Low and V. Ntziachristos, *Nat. Med.*, 2011, **17**, 1315; (*c*) Q. T. Nguyen, E. S. Olson, T. A. Aguilera, T. Jiang, M. Scadeng, L. G. Ellies and R. Y. Tsien, *Proc. Natl. Acad. Sci. U. S. A.*, 2010, **107**, 4317; (*d*) Y. Urano, M. Sakabe, N. Kosaka, M. Ogawa, M. Mitsunaga, D. Asanuma, M. Kamiya, M. R. Young, T. Nagano, P. L. Choyke and H. Kobayashi, *Sci. Transl. Med.*, 2011, **3**, 110ra119; (*e*) X. Wu, Y. Tian, M. Yu, B. Lin, J. Han and S. Han, *Biomater. Sci.*, 2014, DOI: 10.1039/c4bm00028e.

2 (*a*) H. Kobayashi and P. L. Choyke, *Acc. Chem. Res.*, 2011, **44**, 83; (*b*) H. Kobayashi, M. Ogawa, R. Alford, P. L. Choyke and Y. Urano, *Chem. Rev.*, 2010, **110**, 2620; (*c*) H. Lee, W. Akers, K. Bhushan, S. Bloch, G. Sudlow, R. Tang and S. Achilefu, *Bioconjugate Chem.*, 2011, **22**, 777.

3 (*a*) E. B. Dickerson, E. C. Dreaden, X. Huang, I. H. El-Sayed, H. Chu, S. Pushpanketh, J. F. McDonald and M. A. El-Sayed, *Cancer Lett.*, 2008, **269**, 57; (*b*) X. Huang, P. K. Jain, I. H. El-Sayed and M. A. El-Sayed, *Lasers Med. Sci.*, 2008, **23**, 217; (*c*) X. Liu, H. Tao, K. Yang, S. Zhang, S. T. Lee and Z. Liu, *Biomaterials*, 2011, **32**, 144; (*d*) X. Huang, I. H. El-Sayed, W. Qian and M. A. El-Sayed, *J. Am. Chem. Soc.*, 2006, **128**, 2115; (*e*) K. Yang, S. Zhang, G. Zhang, X. Sun, S. T. Lee and Z. Liu, *Nano Lett.*, 2010, **10**, 3318; (*f*) L. R. Hirsch, R. J. Stafford, J. A. Bankson, S. R. Sershen, B. Rivera, R. E. Price, J. D. Hazle, N. J. Halas and J. L. West, *Proc. Natl. Acad. Sci. U. S. A.*, 2003, **100**, 13549; (*g*) J. Chen, C. Glaus, R. Laforest, Q. Zhang, M. Yang, M. Gidding, M. J. Welch and Y. Xia, *Small*, 2010, **6**, 811; (*h*) J. Yang, J. Choi, D. Bang, E. Kim, E. K. Lim, H. Park, J. S. Suh, K. Lee, K. H. Yoo, E. K. Kim, Y. M. Huh and S. Haam, *Angew. Chem.,Int. Ed.*, 2011, **50**, 441; (*i*) J. Zhou, Z. Lu, X. Zhu, X. Wang, Y. Liao, Z. Ma and F. Li, *Biomaterials*, 2013, **34**, 9584.

4 (*a*) M. Chen, X. Fang, S. Tang and N. Zheng, *Chem. Commun.*, 2012, **48**, 8934; (*b*) K. Yang, H. Xu, L. Cheng, C. Sun, J. Wang and Z. Liu, *Adv. Mater.*, 2012, **24**, 5586; (*c*) Z. Zha, X. Yue, Q. Ren and Z. Dai, *Adv. Mater.*, 2013, **25**, 777.

5 (*a*) Z. Li, Y. Song, Y. Yang, L. Ynag, X. Huang, J. Han and S. Han, *Chem. Sci.*, 2012, **3**, 2941; (*b*) X. Wu, Y. Tian, M. Yu, J. Han and S. Han, *Biomater. Sci.*, 2014, **2**, 972.

6 J. Y. Hong, H. Yoon and J. Jang, *Small*, 2010, **6**, 679.

7 T. Yoshimori, A. Yamamoto, Y. Moriyama, M. Futai and Y. Tashiro, *J. Biol. Chem.*, 1991, **266**, 17707.